Journal of Chromatography, 545 (1991) 239–248
Elsevier Science Publishers B.V., Amsterdam

CHROM. 23 163

Selection of the background electrolyte composition with respect to electromigration dispersion and detection of weakly absorbing substances in capillary zone electrophoresis

VLADIMÍR ŠUSTÁČEK, FRANTIŠEK FORET and PETR BOČEK*

Institute of Analytical Chemistry, Czechoslovak Academy of Sciences, Veveří 97, CS-61142 Brno (Czechoslovakia)

ABSTRACT

A characteristic feature of the migration of sample ions in zone electrophoresis is the formation of either fronting or tailing zones. This so-called electromigration dispersion can generally be suppressed by keeping the sample concentration more than two orders of magnitude below the concentration of the background electrolyte (BGE). In capillary zone electrophoresis the low sample concentration decreases the reliability of on-column UV absorbance detection, especially when substances having low molar absorption coefficients are to be detected. By the proper selection of the electrophoretic mobility of the background electrolyte co-ion, both electromigration dispersion and detection can be optimized. The migration behaviour of phenyllactic acid and four phenyl derivatives of acetic acid was studied in buffered electrolytes with different mobilities and concentrations of the BGE co-ions. For a better understanding of zone broadening, a simplified model of the electromigration together with some model calculations is presented.

INTRODUCTION

On-column UV absorbance detection is the most universal detection method used in capillary zone electrophoresis (CZE). As the optical path length, given by the inside diameter of the separation capillary used, is short (typically 50 μm), it is desirable to keep the concentration of separated ions as high as possible to obtain a good detector response. This requirement concerns especially substances having low molar absorption coefficients. However, an increase in the concentration of the sample ions results in an increase in the electromigration dispersion [1] and, consequently, to a decrease in the separation efficiency.

The electromigration dispersion is related to changes in the local electric field strength in a migrating zone with respect to that in the background electrolyte (BGE). It can be characterized by the electric field strength, which is variable with time and length inside an individual zone. The result is obvious: each part of an individual zone moves with its own velocity and, moreover, the situation changes with time and length. The resulting dispersion may in some instances be so strong that it plays a dominant role among other dispersive factors (for their characterization, see ref. 2).

0021-9673/91/$03.50

In current practice, the electromigration dispersion is frequently suppressed by working under conditions such that the concentration of a solute is lower than that of the BGE by more than two orders of magnitude [1]. Obviously, there are two ways to fulfil such a condition: to inject a small amount of a dilute sample or to use a high-concentration background electrolyte.

Of course, both of the above-mentioned procedures have their limitations. When weakly absorbing solutes are detected by using a UV absorption detector, the sample concentration cannot be reduced below the sensitivity of the detector used. A substantial increase in the concentration of BGE minimizes the electromigration dispersion but simultaneously causes a considerable increase in the BGE conductivity. Then the voltage driving the separation must be decreased to avoid column overheating, which results in a longer analysis time.

The importance of the composition of the BGE for improving the zone sharpness has been already noted by Hjertén *et al.* [3,4]. In this paper, a study of the effect of the difference between the effective mobilities of a solute and of the BGE co-ion on the electromigration dispersion is reported. It is shown theoretically and has been verified experimentally that the electromigration dispersion can be reduced substantially by the proper selection of the composition of the BGE regarding the mobilities of the solute and of the BGE co-ion.

THEORETICAL

The problem of unsteady-state migration (electromigration dispersion) was first solved by Weber [5] for strong electrolytes, and this approach has recently been extended to cover also the migration of a sample pulse (for a review, see ref. 6). Another solution to this problem has been published by Virtanen [7] and Mikkers *et al.* [1].

The core of the calculation presented here is based on Weber's solution, which is modified for weak uni–univalent electrolytes. Absolute values of mobilities are used in all calculations (*i.e.*, $u_i > 0$ for both cations and anions) and both ionic and effective mobilities are assumed to be constants (*i.e.*, both temperature and pH are assumed to be constant at any time and capillary length). The capillary is filled with the background electrolyte AR, the specific conductivity of which is given by the relationship

$$\kappa_0 = Fc_{A,0}(u_A + u_R) = F\bar{c}_{A,0}\bar{u}_A \cdot \frac{u_A + u_R}{u_A} \tag{1}$$

For the specific conductivity in a migrating sample zone, it analogously holds that

$$\kappa_S = F\left(\bar{c}_A\bar{u}_A \cdot \frac{u_A + u_R}{u_A} + \bar{c}_S\bar{u}_S \cdot \frac{u_S + u_R}{u_S}\right) \tag{2}$$

The adjustment of the concentrations in migrating zones may be described by the Kohlrausch regulating function in the forms [8–10]

$$\omega_0 = \bar{c}_{A,0} \cdot \frac{u_A + u_R}{u_A} \tag{3}$$

$$\omega_S = \bar{c}_A \cdot \frac{u_A + u_R}{u_A} + \bar{c}_S \cdot \frac{u_S + u_R}{u_S} \tag{4}$$

The well known condition $\omega_S = \omega_0$ gives the equation

$$\bar{c}_{A,0} \cdot \frac{u_A + u_R}{u_A} = \bar{c}_A \cdot \frac{u_A + u_R}{u_A} + \bar{c}_S \cdot \frac{u_S + u_R}{u_S} \tag{5}$$

The solution of the system of the partial differential transport equations for components A and S is known in the form [5,8]

$$\omega_S/\kappa_S = \sqrt{a/b} \tag{6}$$

where

$$a = \omega_0 l/(F\bar{u}_A\bar{u}_S) \tag{7}$$

and

$$b = jt \tag{8}$$

By combining eqns. 5 and 6, explicit equations for the sample concentration in a migrating sample zone is obtained:

$$\bar{c}_S(l,t) = \frac{\bar{c}_{A,0}}{\bar{u}_S - \bar{u}_A} \cdot \frac{u_S}{u_S + u_R} \cdot \frac{u_A + u_R}{u_A} \left(\frac{1}{F}\sqrt{\frac{b}{a}} - \bar{u}_A \right) \tag{9}$$

Similarly, for the concentration of the BGE co-ion in the sample zone it holds that

$$\bar{c}_A(l,t) = \frac{\bar{c}_{A,0}}{\bar{u}_S - \bar{u}_A} \left(\bar{u}_S - \frac{1}{F}\sqrt{\frac{b}{a}} \right) \tag{10}$$

Eqn. 9 covers both the cases $\bar{u}_S > \bar{u}_A$ and $\bar{u}_S < \bar{u}_A$; characteristic profiles for both cases are depicted in Fig. 1. Obviously, for $\bar{u}_S > \bar{u}_A$ the profile of $\bar{c}_S$ in the capillary is concave and the peak detected is convex, and for $\bar{u}_S < \bar{u}_A$ the opposite apply. In practice, of course, the use of a fixed detector is the most important means of detection and, therefore, the profile of $\bar{c}_S(t)$ at a fixed point $l = L$ will be further described.

Eqn. 9 describes the profile generated by the electromigration between two neighbouring fronts of electrolytes SR and AR [5,8], where the maximum of $\bar{c}_S$ corresponds to the adjusted Kohlrausch value given by eqn. 5 for $\bar{c}_A = 0$:

$$\bar{c}_{S,0} = \bar{c}_{A,0} \cdot \frac{u_S}{u_S + u_R} \cdot \frac{u_A + u_R}{u_A} \tag{11}$$

In practice, however, the maximum $\bar{c}_S$ value seldom reaches the concentration $\bar{c}_{S,0}$ and

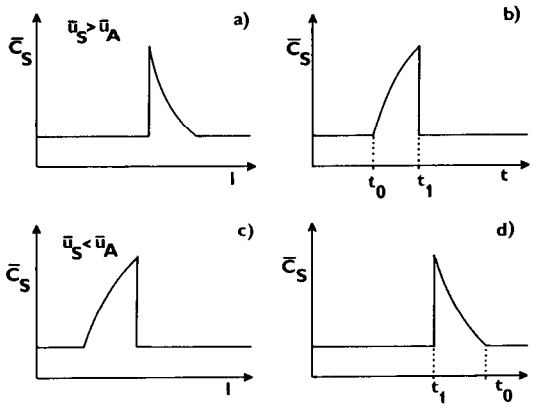

Fig. 1. Scheme of the shapes of the concentration profiles due to electromigration dispersion (see eqn. 9). (a),(b) $\bar{u}_S > \bar{u}_A$; (c),(d) $\bar{u}_S < \bar{u}_A$; (a),(c) $\bar{c}_S = f(l)$, inside the capillary at a given time; (b),(d) $\bar{c}_S = f(t)$, peaks recorded by a fixed-point detector.

is given by the amount injected. To determine the actual maximum $\bar{c}_S$ value in a detected peak, one may integrate the $\bar{c}_S(t)$ profile and compare it with the amount of sample injected.

The calculation of the sample zone profile is started at the time

$$t_0 = L\kappa_0/(\bar{u}_S j) \tag{12}$$

which represents the migration time of a single ion S in the background electrolyte (see scheme in Fig. 1). The profile is then numerically integrated to obtain the amount of substance S in the zone:

$$n_S(\text{calc.}) = \phi \int_{t_0}^{t_1} \bar{c}_S(t) v_S(t) \mathrm{d}t \tag{13}$$

and the calculation is stopped at time t_1 when $n_S(\text{calc.}) \geqslant n_S(\text{injected})$. The velocity of the migration of a concentration $\bar{c}_S(t)$ at the detection time t is given by the expression

$$v_S(t) = \bar{u}_S j/\kappa(t) \tag{14}$$

where $\kappa(t)$ is the specific conductivity in the detection point at the time t given by eqn. 2.

By multiplication of the calculated concentration profile $\bar{c}_S(t)$ with absorption coefficient of species S, one can simulate the record of electrophoretic analysis with UV detection.

To obtain a simple explicit relationship between the peak width and the effective mobilities of A and S, another approximation should be introduced. Let us assume that the solute concentration in the peak maximum, $\bar{c}_{S,max}$ has for a constant amount of sample injected a constant value proportional to $\bar{c}_{S,0}$ (given by eqn. 11):

$$\bar{c}_{S,max} = B\bar{c}_{S,0} \tag{15}$$

where $B < 1$ is a constant. Then the time t_1 when the peak maximum passes through the detector can be expressed as

$$t_1 = t_0 \cdot \frac{[B(\bar{u}_S - \bar{u}_A) + \bar{u}_A]^2}{\bar{u}_A^2} \tag{16}$$

As in capillary electrophoresis the peak width in a time-based record is a function of analysis time (less mobile zone passes through the detection cell for a longer time) [9], the zone widths related to the time in which the peak maximum was detected should be compared instead of the zone widths only. From eqn. 16, the relative sample zone width at the baseline is given by

$$\frac{t_1 - t_0}{t_0} = 2B \cdot \frac{\bar{u}_S - \bar{u}_A}{\bar{u}_A} + B^2\left(\frac{\bar{u}_S - \bar{u}_A}{\bar{u}_A}\right)^2 \tag{17}$$

It is obvious that the relative zone width due to electromigration dispersion is proportional to the difference $\bar{u}_S - \bar{u}_A$. In practice, the actual peak width measured also includes the contributions due to a finite sample pulse at the injection point, due to diffusion, etc., which should be added to the right-hand side of eqn. 17.

EXPERIMENTAL

Apparatus

Experiments were performed in laboratory-made equipment described in detail previously [11]. The separation column was a 46 cm × 75 μm I.D. fused-silica capillary (SGE, Austin, TX, U.S.A.); the inner surface of the capillary was coated with linear polyacrylamide [12] to suppress electroosmotic flow during analysis. Sample introduction was performed by hydrodynamic flow from the sample vial, raised 5 cm above the liquid level in the electrode vessels. The capillary was rinsed with the background electrolyte after each run.

On-column UV detection at 254 nm was used, employing a laboratory-made single-beam detector with an optically stabilized low-pressure mercury lamp. The noise of the detector was *ca.* $3 \cdot 10^{-4}$ absorbance. A fibre-optic detection cell located 41 cm from the injection end of the capillary was described previously [13].

Absorption coefficients at 254 nm were measured by means of a Varian Series 634 spectrophotometer with the use of 1-cm cuvettes and *ca.* $2 \cdot 10^{-4}$ *M* solutions of each compound. All calculations were made on a PMD-85-2 microcomputer (Tesla, Bratislava, Czechoslovakia).

Chemicals

Glutamic acid (Lachema, Brno, Czechoslovakia), 2-hydroxyisobutyric acid (Fluka, Buchs, Switzerland), trichloroacetic acid (Merck, Darmstadt, Germany) and 4-aminobutyric acid (Serva, Heidelberg, Germany), all of analytical-reagent grade, were used for the preparation of the background electrolytes. Phenyl-substituted acids (Fluka), purum grade, served as model sample components. The pH of the sample solution was adjusted to 4.0 with 4-aminobutyric acid.

RESULTS AND DISCUSSION

Phenyllactic acid and four phenyl derivatives of acetic acid were used for the experimental evaluation of the role of the electromigration dispersion on separation and detection in CZE. The electrophoretic mobilities of the sample components are listed in Table I together with their absorption coefficients and concentrations in the sample injected into the capillary. The physico-chemical constants of the substances used for the preparation of the background electrolytes are summarized in Table II.

Based on preliminary experiments, pH 4.0 was selected as the optimum for the separation; at this pH, all sample components are well separated. As no reliable data on mobilities and pK values were available, the effective mobilities were determined experimentally from migration times of single compounds injected, using BGE D (see Table III) and a voltage of 10 kV. No electroosmotic flow was observed under these conditions.

As the molar absorption coefficients ε of all phenyl-substituted acids studied lie in the region of 220–630 l/mol · cm at 254 nm, the absorbance of the zones in the separation capillary was too low and their detection was possible only when high concentrations of solutes in their zones were ensured.

The role of the composition of the BGE on the separation and detection can be explained with the aid of the experimental separation records shown in Fig. 2. Fig. 2a shows the electrophoretic analysis of the model mixture in the background electrolyte containing trichloroacetate as a co-ion, the effective mobility of which is several times higher than those of the sample components (see Tables I and II). Obviously, the analysis is poor, the peaks being very wide and not resolved from one another.

Fig. 2b shows the same electrophoretic analysis in the electrolyte having the same components but ten times higher concentrations. In this instance the peaks of sample substances were still deformed, but their baseline resolution was achieved. As this BGE has a high specific conductivity, the separation voltage had to be decreased to prevent overheating. Excessive heating due to a high current density was observed especially in the low-conductivity sample pulse at the injection end of the capillary. A large temperature rise in this pulse (which took 1.4 cm of the capillary in this experiment) may cause peak broadening during the preconcentration at the sample pulse/BGE

TABLE I

PHENYL-SUBSTITUTED ACIDS USED FOR THE PREPARATION OF THE MODEL SAMPLE

Effective mobilities were determined experimentally from migration data; the ionic mobility of phenylacetic acid was taken from ref. 14 as a mean of reported values; the other ionic mobilities were calculated according to related compounds with the help of ref. 14; ε = absorption coefficient; c = concentration of the substance in the sample.

Substance	Abbreviation	Effective mobility (10^{-5} cm^2/V s)	Ionic mobility (10^{-5} cm^2/V s)	ε (l/mol · cm)	c (mmol/l)
3-Phenyllactic acid	PL	17.4	*ca.* 25	230	4
Phenylacetic acid	PA	10.4	*ca.* 30	220	4
2-Hydroxyphenylacetic acid	2-HPA	8.9	*ca.* 30	630	2
3-Hydroxyphenylacetic acid	3-HPA	9.9	*ca.* 30	480	2
4-Hydroxyphenylacetic acid	4-HPA	8.2	*ca.* 30	350	2

TABLE II

SUBSTANCES USED FOR THE PREPARATION OF THE BACKGROUND ELECTROLYTES

Ionic mobilities and pK_a values were taken from ref. 14; effective mobilities at pH = 4.0 were calculated by multiplying ionic mobilities by the respective degree of ionization.

Substance	pK_a	Ionic mobility (10^{-5} cm^2/V s)	Effective mobility (10^{-5} cm^2/V s)
Trichloroacetic acid	0.64	36.2	36.2
2-Hydroxyisobutyric acid	3.97	33.5	17.3
Glutamic acid	4.32	27.0	8.7
4-Aminobutyric acid (counter ion)	4.0	*ca.* 34	*ca.* 17

boundary and, consequently, deterioration of the analysis. Also, an analysis time several times longer than in the previous instance is a clear disadvantage of such an approach when using capillaries with I.D. greater than *ca.* 10 μm.

Analyses in electrolytes with a lower effective mobility of the BGE co-ion are shown in Fig. 2c and d. In both instances the resolution of zones was sufficient and the analysis time was the same as in that shown in Fig. 2a. The sharpest peaks with the maximum heights are those of components having an effective mobility close to that of the background electrolyte. As the effective mobilities of most sample components are not too different from that of glutamate, the use of electrolyte D is optimum for the separation of the mixture of phenyl-substituted acids.

The use of a low-mobility glutamate co-ion also brings another advantage. The

TABLE III

EXPERIMENTAL CONDITIONS IN CZE ANALYSES OF THE MODEL MIXTURE OF PHENYL-SUBSTITUTED ACIDS

These experimental conditions were applied in CZE analyses shown in Fig. 2a–d and were then used as input data for the simulations, the results of which are shown in Fig. 3a–d.

Fig.	BGE	Sample volume (nl)	Current (μA)	Voltage (kV)
2a, 3a	A	30	16	16
2b, 3b	B	60	40	6
2c, 3c	C	30	15	16
2d, 3d	D	30	12	16

Composition of background electrolytes[a].

BGE	Co-ion constituent	Concentration (mol/l)
A	Trichloroacetic acid	0.01
B	Trichloroacetic acid	0.1
C	2-Hydroxyisobutyric acid	0.02
D	Glutamic acid	0.03

[a] 4-Aminobutyric acid was added to pH 4.0 in all instances.

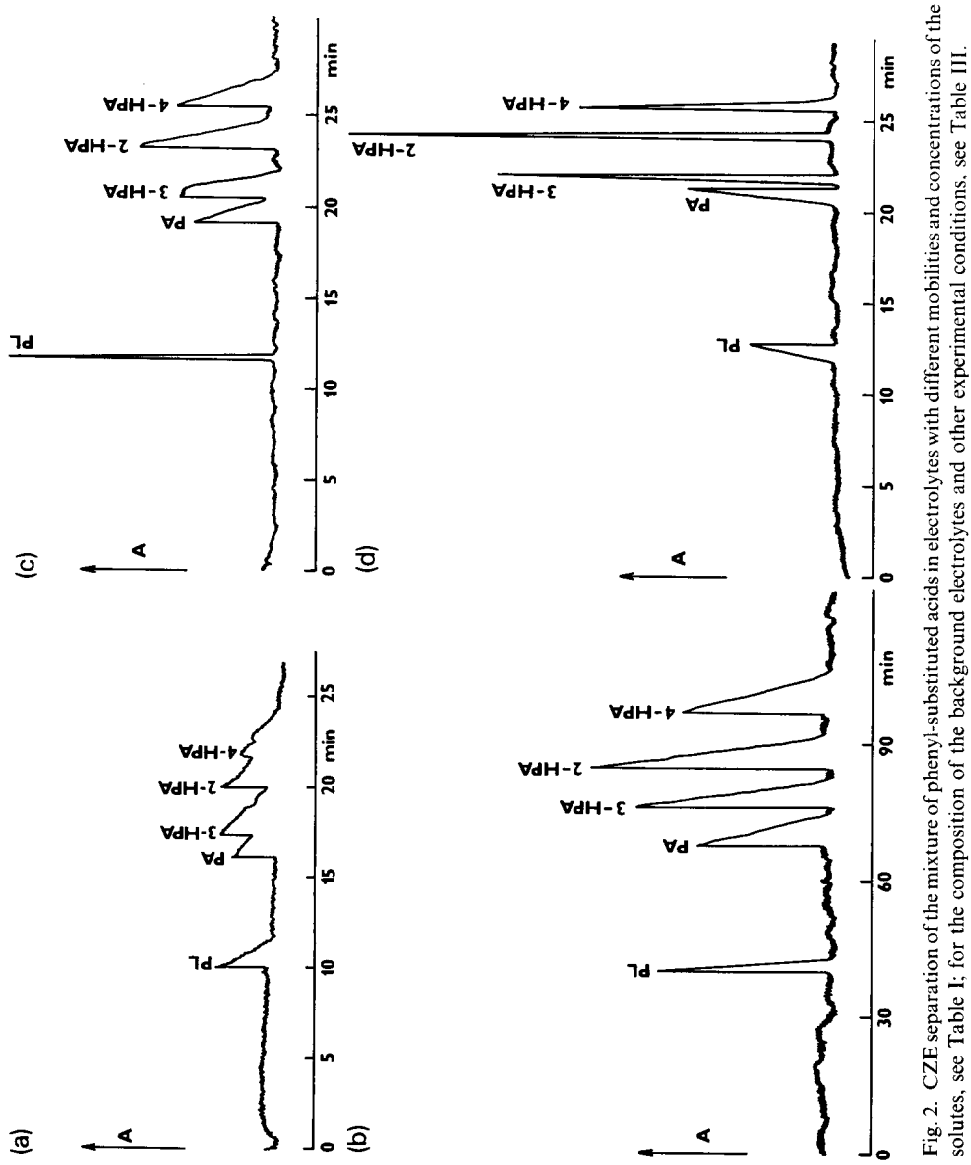

Fig. 2. CZE separation of the mixture of phenyl-substituted acids in electrolytes with different mobilities and concentrations of the BGE co-ions. For abbreviations of solutes, see Table I; for the composition of the background electrolytes and other experimental conditions, see Table III.

BGE can contain a higher concentration of such a co-ion than that of a co-ion with a higher mobility and the specific conductivity of the BGE does not change. A higher co-ion concentration results in decreased electromigration dispersion without increasing thermal effects. In our experiments, the concentrations of electrolytes C and D were higher than that of BGE A to ensure that the specific conductivities of these three electrolytes were approximately the same (*i.e.*, thermal effects in CZE analyses were not too different and the mobilities can be considered to be constant).

Fig. 3 shows simulated electrophoregrams of the analyses shown in Fig. 2, calculated according to the procedure described under Theoretical. If the experimental and simulated records are compared, it is seen that they coincide very well in spite of the fact that many simplifications have been made in the theory presented. Large deviations occur only in the calculated migration times. The differences are caused by neglect of the contribution of H^+ ions to the specific conductivity (which was more than 5% of κ_0 of electrolytes A, C and D), and, especially, by neglecting the increase in

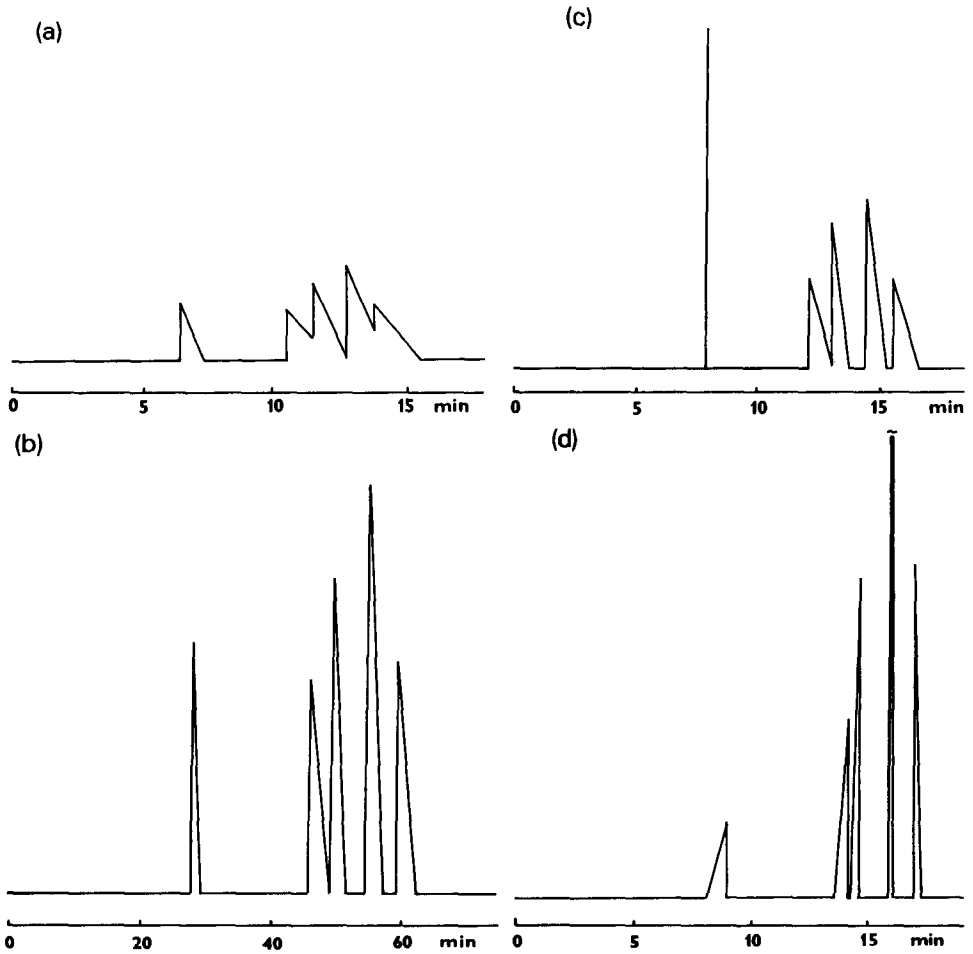

Fig. 3. Simulated records of CZE analyses shown in Fig. 2.

temperature inside the capillary due to Joule heating. It is known that ionic mobilities increase by about 2% if the temperature increases by 1°C. If mobilities of all ions (sample ion, co-ion, counter ion) increase to the same extent, the character of the analysis record does not change and only the migration times vary.

Another large difference between the calculated and experimental records concerns peaks of solutes having effective mobilities almost the same as that of the BGE co-ion. In this instance the other contributions to the peak width, such as a finite length of a sample pulse at the injection point and diffusion, are comparable to the electromigration dispersion and cause additional peak broadening.

It is clear from this study that the selection of the composition of the BGE has a crucial impact on the separation and detection sensitivity in all instances where weakly absorbing substances are to be detected. The simple theoretical model presented here can help one to find optimum separation conditions for analysing such substances.

SYMBOLS

t time
l length coordinate
L length of the separation capillary (from sampling point to detector)
ϕ internal cross-sectional area of the capillary
j current density
F Faraday constant
u_i ionic mobility of species i
$\bar{u}_i$ effective mobility of species i
c_i ionic concentration
$\bar{c}_i$ total (analytical) concentration
$\bar{c}_{A,0}$ analytical concentration of co-ion A in the BGE

Subscripts
S sample component
A BGE co-ion constituent
R BGE counter ion

REFERENCES

1 F. E. P. Mikkers, F. M. Everaerts and Th. P. E. M. Verheggen, *J. Chromatogr.*, 169 (1979) 1.
2 F. Foret, M. Deml and P. Boček, *J. Chromatogr.*, 452 (1988) 601.
3 S. Hjertén, *Top. Bioelectrochem. Bioenerg.*, 2 (1978) 89.
4 S. Hjertén, K. Elenbring, F. Kilár, J. Liao, A. J. C. Chen, C. J. Siebert and M. Zhu, *J. Chromatogr.*, 403 (1987) 47.
5 H. Weber, *Die Partiellen Differential Gleichungen der Mathematischen Physik*, Vol. I, Friedrich Vieweg u. Sohn, Braunschweig, 1910.
6 F. Foret and P. Boček, in A. Chrambach (Editor), *Advances in Electrophoresis*, Vol. 3, VCH, Weinheim, 1989, pp. 271–347.
7 R. Virtanen, *Acta Polytech. Scand.*, 123 (1974) 1.
8 P. Gebauer, M. Deml, J. Pospíchal and P. Boček, *Electrophoresis*, 11 (1990) 724.
9 W. Thormann, R. A. Mosher and M. Bier, *Electrophoresis*, 6 (1985) 78.
10 L. M. Hjelmeland and A. Chrambach, *Electrophoresis*, 3 (1982) 9.
11 S. Fanalli, L. Ossicini, F. Foret and P. Boček, *J. Microcolumn Sep.*, 1 (1989) 190.
12 S. Hjertén, *J. Chromatogr.*, 347 (1985) 191.
13 F. Foret, M. Deml, V. Kahle and P. Boček, *Electrophoresis*, 7 (1986) 430.
14 J. Pospíchal, P. Gebauer and P. Boček, *Chem. Rev.*, 89 (1989) 419.